IOPscience iopscience.iop.org

Home Search Collections Journals About Contact us My IOPscience

Magnetic phase diagrams of neodymium

This article has been downloaded from IOPscience. Please scroll down to see the full text article.

1991 J. Phys.: Condens. Matter 3 8079

(http://iopscience.iop.org/0953-8984/3/41/007)

View the table of contents for this issue, or go to the journal homepage for more

Download details:
IP Address: 171.66.16.147
The article was downloaded on 11/05/2010 at 12:37

Please note that terms and conditions apply.

J. Phys.: Condens. Matter 3 (1991) 8079–8094. Printed in the UK

Magnetic phase diagrams of neodymium

S W Zochowski†, K A McEwen† and E Fawcett‡

† Department of Physics, Birkbeck College, University of London, Malet Street, London WC1E 7HX, UK

‡ Physics Department, University of Toronto, Toronto, Canada M5S 1A7

Received 9 August 1991

Abstract. The magnetic phase diagrams of Nd, for fields up to 12 T applied parallel to the crystallographic *a*-, *b*-, and *c*-directions, have been constructed from observed anomalies in thermal expansion and longitudinal magnetostriction measurements. The results are interpreted with reference to neutron diffraction studies and in terms of multi-domain single-*q*, double-*q*, triple-*q* and quadruple-*q* structures.

1. Introduction

Early specific heat measurements on Nd [1] first indicated the existence of magnetic phase transitions at $T \approx 19$ K and 7.5 K. The results of the first neutron diffraction studies [2] were interpreted in terms of an antiferromagnetic structure in which the moments are sinusoidally modulated with a period incommensurate with the lattice. Because of the DHCP structure of Nd, atoms in alternating layers find themselves in either a nearly hexagonal or a nearly cubic environment. The moments were thought to order, parallel to the basal plane, on the hexagonal sites at the higher temperature and on the cubic sites at the lower temperature. Subsequent experiments indicated that the magnetic structure of Nd was considerably more complex and a detailed understanding has proved to be rather elusive. Although neutron diffraction studies of Nd have revealed a sequence of modulated magnetic structures below the Néel temperature of 19.9 K [3], this technique is not necessarily the most appropriate to delineate all of the phase transitions in the *(H,T)* plane. We have therefore combined thermal expansion, magnetostriction and magnetization measurements to detect the phase transitions and map out the magnetic phase diagrams of Nd. This paper presents the results of a comprehensive investigation, which we have interpreted in terms of multi-domain single-*q*, double-*q*, triple-*q* and quadruple-*q* magnetic structures [2,4–7].

In zero magnetic field, Nd undergoes a sequence of magnetic structural changes, as outlined below. A schematic representation of the consequent magnetic satellites observed by neutron diffraction around the (100) Bragg reflection at various temperatures and in zero applied magnetic field is shown in figure 1. Immediately below T_N, six magnetic satellites appear around a general reciprocal point along the three equivalent crystallographic *b*-directions ($\langle 100 \rangle$ in reciprocal space) at wavevectors $\pm q_{h1}$, $\pm q_{h2}$, $\pm q_{h3}$ of equivalent magnitude $0.147|\tau_{100}|$. This pattern may be interpreted in terms of separate magnetic domains within each of which the magnetization density

0953-8984/91/418079+16$03.50 © 1991 IOP Publishing Ltd

is spatially modulated with one of the wavevectors $\pm q_i$. This is the 'single-q' state. Alternatively, a 'multiple-q' state, such as those having 'double-q' and 'triple-q' structures, may exist; these are made up of linear combinations of the symmetry related modulations of the magnetization. Renormalization-group analysis [4] indicated that the magnetic structure would be triple-q, rather than single-q, if the Néel phase transition were second order. The neutron diffraction data available in 1978 indicated that the transition was continuous and it was concluded that the transition was to a triple-q structure [3]. However, our subsequent thermal expansion results [8] revealed that the Néel transition at $T_N = 19.95$ K is, in fact, first order. This evidence, together with neutron diffraction experiments in a magnetic field [6], identifies the Néel transition as to a single-q state. Just below T_N, at $T_2 = 19.1$ K, a second first-order transition was observed in zero-field thermal expansion measurements [8]. This transition is attributed to a single-q to double-q transition at which the wavevectors rotate away from $\langle 100 \rangle$, producing an array of 12 satellites [9]. The ordering of the moments at T_N and T_2 is ascribed primarily to the hexagonal sites. A free-energy analysis which permits an understanding of the 'high-temperature' transitions at T_N and T_2 has been given [10, 11].

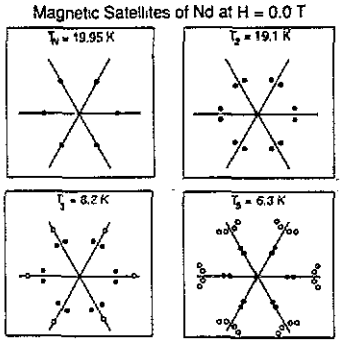

Figure 1. Schematic representation of the magnetic satellite reflections observed around (100) at various temperatures and in zero applied magnetic field. The filled and open circles denote the *hexagonal* and *cubic* satellites, respectively.

Further transitions have been observed below 9 K in zero magnetic field, as shown in figure 1. At $T_3 \approx 8.2$ K, a transition is marked by the appearance of satellites near $0.18\tau_{100}$; this ordering is ascribed primarily to the moments on the cubic sites.

The length of the wavevectors associated with the ordering on the hexagonal sites decreases steadily with decreasing temperature and is $\approx 0.12|\tau_{100}|$ just above $T_5 \approx 6.3$ K. The transition at T_5 involves the longitudinal splitting of these satellites along the {100} axes into pairs, with $q_1 = 0.106\tau_{100}$ and $q_2 = 0.116\tau_{100}$ [12]; simultaneously, the satellites near $0.18\tau_{100}$ split transversely along {010} directions into four peaks, which we shall describe by q_3 and q_4 [7, 13]. The fourfold splitting of the $0.18\tau_{100}$ satellites was first detected by B Lebech [unpublished, ca. 1981] but the simultaneity with the longitudinal splitting of the $0.12\tau_{100}$ satellites was not observed until later. The consequent array of 36 satellites observed below T_5 is illustrated in figure 1. It has been shown [7] that this diffraction pattern arises from the six domains of a quadruple-q structure with four inequivalent wavevectors. Such a structure may be regarded as a coupling of two closely-related pairs of inequivalent wavevectors associated with the hexagonal and cubic layers. Although it is convenient to refer to

q_1 and q_2 as *hexagonal* satellites and q_3 and q_4 as *cubic* satellites respectively, detailed analysis of the satellite intensities indicates the presence of small induced moments with wavevectors q_1 and q_2 on the *cubic* sites and also moments with wavevectors q_3 and q_4 on the *hexagonal* sites [13]. The splitting of the satellites at T_5 marks the onset of this quadruple-q structure.

Below T_5, no other changes in the diffraction pattern have yet been observed which may be associated with other transitions.

Until recently, neutron diffraction studies in an applied magnetic field have been performed solely in the high-temperature region from 10 K to 18 K [6] and at 4.2 K [12, 14, 15]. Domain re-orientation has been observed at fields $H < 1.0$ T and further transitions have been observed near $H = 2.5$ T and 3.0 T. The measurements in the high-temperature region provided the first definitive evidence for the double-q model, by showing that a single domain of the double-q structure was produced in a field of 0.8 T. Furthermore, a double-q to single-q transition was observed at approximately 2.6 T [6, 11].

Phase transitions have also been observed by techniques other than neutron diffraction. Four anomalies in heat capacity measurements were seen between 2 K and 10 K, in zero magnetic field [16]. On heating, these peaks were observed at 5.8 K, 6.3 K, 7.8 K, and 8.3 K. Elastic constants have been measured in zero magnetic field in the temperature range 4.2 to 300 K [17] and the magnetic-field dependence of the elastic constants of Nd for fields $H < 8$ T has been examined at 4.2 K [18]. AC susceptibility measurements showed evidence of transitions at 6.3 K, 7.8 K and 8.3 K [19]. A partial phase diagram of Nd was constructed from magnetization measurements, up to 5 T, below 14 K [20]. There has been no report of a dilatation study of Nd, except that of our earlier work [8].

2. Experimental details

A 4 mm cube single crystal of Nd, prepared by Dr D Fort at the Department of Metallurgy, University of Birmingham, was used in this study. This sample was previously used in neutron diffraction [6] and dilatation [8] experiments. The faces of the sample were cut perpendicular to the crystallographic a-, b- and c-directions.

Meaurements of strain were made relative to the body of a Cu–Be capacitance dilatometer, which relied on arrangements of parallel springs [21] for its design [22]. Inherent limitations of the dilatometer meant that constant-field measurements could be taken with increasing temperature only. The capacitance was measured using a General Radio Model 1616 Precision Capacitance Bridge in conjunction with a Model 1316 Oscillator, a 1236 Detector, and a DEC MINC-11 minicomputer. The capacitance changes were converted to length changes using White's formula, which corrects for the distortion of the electric field near the edge of the capacitor electrode [23]. The temperature was measured using a calibrated carbon-glass sensing element. For field-dependent thermal expansion and magnetostriction measurements, a magnetic field with $H < 12$ T was applied parallel to the measurement direction.

We have mapped out the magnetic phase diagrams with the applied field parallel to the a-, b-, and c-axes of Nd by identifying anomalies corresponding to the transitions in the thermal expansion and magnetostriction of the sample. The anomalies used to deduce the phase diagrams are indicated by arrows and labelled where appropriate in the figures below. Note that the thermal expansion and magnetostriction

curves have been displaced for convenience of illustration and that their absolute positions are not significant. To ensure that the observed anomalies are due to the sample and are not an artefact of the capacitance cell, additional measurements were made using a sample of high-purity copper. No anomalies were observed in this case.

Magnetization measurements were made at the High Magnetic Field Laboratory (SNCI) of the CNRS-MPI in Grenoble, France. The measurements were made using an integrating-digital-voltmeter induction magnetometer in fields $H < 15$ T and at temperatures between 4.2 K and 300 K.

3. Results

3.1. Thermal expansion

3.1.1. Thermal expansion (a- and b-axes). The results for the thermal expansion in the basal plane of Nd may be presented in two groups: the first group includes the 'high-temperature' transitions near the Néel temperature, and the second group includes the 'low-temperature' transitions which occur below 10 K.

The high-temperature transitions deduced from measurements along the b-axis in zero magnetic field have been dealt with elsewhere [8]. Two first order transitions were clearly visible, one at the Néel temperature, $T_N = 19.95 \pm 0.05$ K and the other at $T_2 = 19.1 \pm 0.1$ K. Two transitions were similarly observed at T_N and T_2 when the thermal expansion was measured along the a-axis. Measurements made in constant magnetic fields also showed anomalies at T_N and T_2, which decreased with increasing field. However, since the heating rate of the sample was relatively high, $dT/dt > 4$ K h^{-1}, these transitions were observed as smooth changes and not as discontinuities.

The second group of transitions, the low-temperature group, occurs between 5 K and 10 K. Thermal expansion results for the a-axis and b-axis are shown in figures 2 and 3, respectively; results for the b-axis have been reported previously [8]. In both zero-field cases, transitions are observed at $T_6 = 5.7$ K, $T_5 = 6.2$ K, and $T_3 = 8.2$ K. These correspond within 0.1 K to the temperatures at which anomalies were seen in heat capacity measurements [16]. T_4 is 7.5 K for the b-axis, but is more difficult to identify in the a-axis data and appears to be at 7.2 K. These temperatures are somewhat lower than the heat capacity value of 7.8 K.

Measurements along the a- and b-axes were also made in constant applied magnetic field; some representative results are shown in figures 2 and 3. The anomalies seen in measurements along the b-axis in low fields, $H < 1$ T, are observed to be almost half as large as those seen in measurements along the a-axis. For $H > 0.6$ T the character of the transition at T_4 changes: in the a-axis case, two transitions are apparent between 5 K and 6 K in $H = 1.43$ T and remain until $H > 2.5$ T. For both the a- and b-axis results, the anomalies seen in the constant-H measurements have disappeared at a field $H > 3.5$ T. Generally, the b-axis anomalies disappear at higher fields than do the corresponding a-axis anomalies.

3.1.2. Thermal expansion (c-axis). It has been established [3,24] that, below $T = 10$ K, the hexagonal sites have induced moments with components along the c-axis due to the ordered moments on the cubic sites and that the cubic sites have induced moments with components in the c-axis due to the ordered moments on the hexagonal sites. We

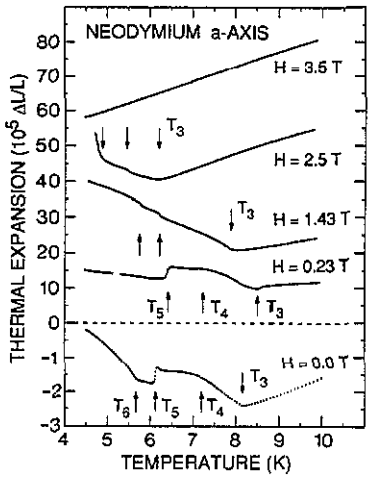

Figure 2. Thermal expansion of Nd, measured along the a-axis, at $H = 0.0, 0.23, 1.43, 2.5$ and 3.5 T. Note the change of scale for $H > 0.0$ T.

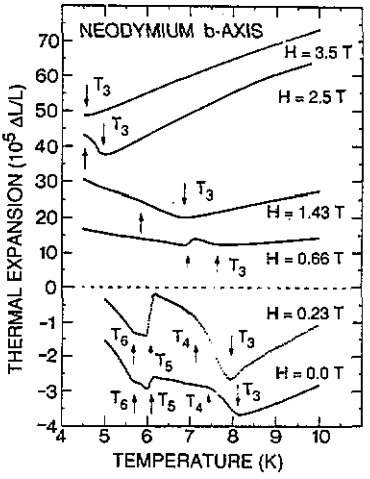

Figure 3. Thermal expansion of Nd, measured along the b-axis, at $H = 0.0, 0.23, 0.66, 1.43, 2.5$ and 3.5 T. Note the change of scale for $H > 0.23$ T.

therefore expect there to be anomalies in the thermal expansion and magnetostriction measured along the c-axis. In fact, the length changes measured along the c-axis are much larger than those measured in the a- and b-directions. The thermal expansion results measured with $H = 0$ and 3.0 T are shown in figure 4.

In zero field, the lattice expands along the c-axis from $T = 4.2$ K to $T_3 = 8.2$ K at which point it contracts until at least $T = 20$ K. No anomalies comparable with those observed along the b- and a-axes were detected around T_2 or T_N. Below 10 K anomalies were observed at $T_6 = 5.7$ K, $T_5 = 6.2$ K, $T_4 = 7.7$ K and $T_3 = 8.2$ K. T_3, T_5 and T_6 agree well with the transition temperatures deduced from the basal plane measurements. T_4 is somewhat higher, and now agrees with the heat capacity result. As the applied magnetic field is increased, the shape of the thermal expansion curve initially exhibits little change, although the temperatures of

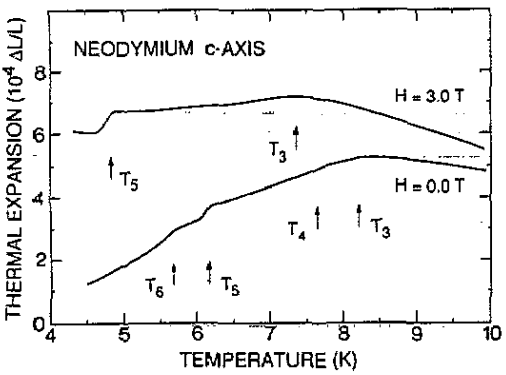

Figure 4. Thermal expansion of Nd, measured along the c-axis, at $H = 0.0$ and 3.0 T.

the anomalies gradually decrease. Above $H = 1$ T the expansion curve flattens out below 10 K, and the transitions can be readily distinguished until well above 4 T, the field at which the transitions faded appreciably along the a- and b-axes. We also note that, in the higher fields, the range of expansivity for $T = 4$ to 10 K is at least an order of magnitude greater in the basal plane.

3.1.3. Thermal expansion (volume). The change in volume in zero magnetic field can be deduced from the results for the a- , b- and c-axes. Results obtained from the high-purity copper sample, together with tabulated results for the expansion coefficient of copper [25], were used to correct the zero-field thermal expansion data for the expansion of the capacitance cell itself. The correction over the range $T = 4.2$ to 10 K is equivalent to a constant positive change in the coefficient of thermal expansion of approximately 1.0×10^{-6} K^{-1}. Figure 5 shows the corrected data for each direction and the calculated result for the change in volume below 10 K. The anomalies in the c-axis direction are seen to be usually in the opposite sense to those along the a- and b-axes, except at T_5, where there is an expansion (on heating) of the lattice in all three directions. Nevertheless, although the c-axis expansion tends to offset the expansion in the basal plane, the volume undergoes transitions at T_6, T_5, T_4 and T_3, with an especially large jump in $\Delta V/V$ at T_5.

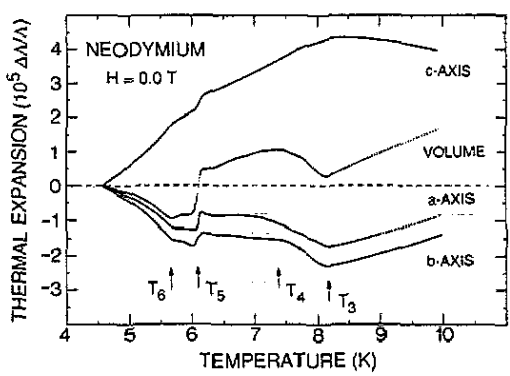

Figure 5. Zero-field corrected thermal expansion results and the volume change, with $\Lambda \equiv L_a, L_b, L_c$ and V.

3.2. Magnetostriction

Magnetostriction measurements along the a-, b- and c-axes were made for various fixed temperatures ranging from 1 to 20 K. In the case of the measurements below 4.2 K, the sample temperature was not allowed to rise above 8 K (i.e., above T_3), and thereby the domain structure produced by the first field run near $T = 1$ K was frozen in. For the measurements made at $T \geqslant 4.2$ K, each field run was made after the sample was heated to $T > T_N$ and then cooled, in zero magnetic field, to the temperature at which the measurement was performed. The magnetostriction measurements were made in both increasing and decreasing magnetic fields. Magnetic hysteresis is evident in all the magnetostriction results and varies in magnitude from 0.1 to 0.5 T. The hysteretic behaviour of the magnetostriction around the field-induced transitions is clearly apparent in the results for fields along the a- and b-axes near $T = 1$ K, shown in figure 6. Hysteresis of the same order of magnitude has been reported in other field-dependent studies [18, 20, 26]. We chose to construct the phase diagrams from the transitions observed in *increasing* field. Field values were normally deduced from the inflection points in the data.

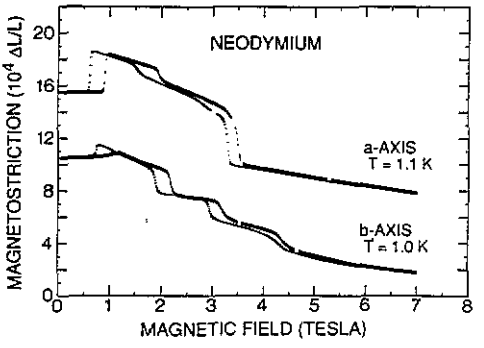

Figure 6. Magnetostriction of Nd, measured along the a- and b-axes, at $T = 1.1$ and 1.0 K, respectively. The vertical and horizontal signatures denote measurements in increasing and decreasing fields, respectively.

3.2.1. Magnetostriction (b-axis). Figure 7 shows representative results from the b-axis magnetostriction measurements. At $T = 1.0$ K, there are clearly transitions at $H_{b1} = 1.1$ T and $H_{b2} = 2.2$ T in increasing field; these are matched by corresponding anomalies at 0.65 and 1.8 T in decreasing field. The transition observed at $H_{b3} = 3.2$ T in increasing field is found at 2.9 T in decreasing field. The next transition may be identified at $H_{b4} = 4.4$ T; the hysteresis continues to lessen as the transition is seen at 4.25 T in decreasing field. There may be a further, weak, transition at 5.7 T, but this one is not obvious in decreasing field. The results for $T = 1.8$ K are very similar. At 2.5 K, only the four transitions at H_{b1} to H_{b4} are apparent at 1.15, 2.2, 3.2 and 4.3 T, i.e., still essentially unchanged. At 3.8 K, the detailed nature of the rapid length changes occuring around H_{b2} becomes more complicated, and it appears that there are now two closely-spaced transitions at $H_{b2} = 2.15$ T and $H_{b2'} = 2.35$ T. We see both H_{b3} and, particularly, H_{b4} beginning to decrease: they now have values of 3.0 and 3.8 T, respectively.

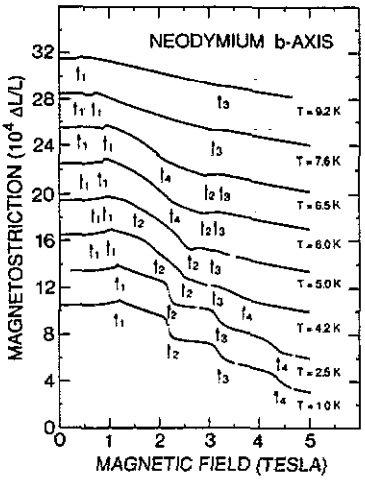

Figure 7. Magnetostriction of Nd, measured in increasing field along the *b*-axis, for various temperatures. The letter '*i*' placed to the right of an arrow refers to the label 'H_{bi}'.

At $T = 4.2$ K, a new feature appears at $H_{b1'} = 0.65$ T below $H_{b1} = 0.95$ T (see figure 7). In decreasing field, the corresponding anomaly occurs almost at zero field, suggesting it is domain-related. The distinction between the transitions at $H_{b2} = 1.95$ T and $H_{b2'} = 2.4$ T has become evident. H_{b3} and H_{b4} persist. The results at 5.0 K are similar, except that H_{b2} and $H_{b2'}$ have become more separated and the transition labelled H_{b4} has almost merged into H_{b3}. By $T = 6.5$ K, the H_{b2} anomaly has disappeared, whereas $H_{b2'}$ has moved closer to H_{b3} and H_{b4} has crossed over $H_{b2'}$ and H_{b3}, i.e., the anomaly near 2.2 T at 6.5 K has the same character as the H_{b4} anomaly at lower temperatures. At 7.6 K, the only remaining high-field anomaly results from an apparent merger of those labelled by $H_{b2'}$ and H_{b3} and is at 3.0 T. At $T = 9.2$ K, only two anomalies can be distinguished, at H_{b1} and H_{b3}. Similar behaviour was found at other temperatures up to 18 K.

3.2.2. Magnetostriction (a-axis). Representative results for *a*-axis magnetostriction are presented in figure 8. Although at $T = 1.1$ K only three transitions are evident along the *a*-axis, at $H_{a1} = 0.9T$, $H_{a2} = 2.0$ T and $H_{a3} = 3.5$ T in increasing field (and at 0.6 T, 1.5 T and 3.25 T, respectively, in decreasing field), they are much more pronounced than in the case of the *b*-axis at this temperature (compare figure 7). At $T = 1.4$ K, the first transition appears to take place in two stages, but this feature is not seen in decreasing field. The situation has changed somewhat at 4.2 K, and there are now clearly two discontinuities below 1 T. Moreover, H_{a2} is now characterised by a small length *increase* in contrast to the *decrease* clearly observed at 1.1 K. The 5.0 K data are very similar, except that the H_{a2} anomaly is weaker; at 5.5 K it can scarcely be resolved. Between 6.0 K and 7.5 K, we now find two sharp transitions below 1 T, and another close to 3 T; the transitions have crossed over as well, so that H_{a2} occurs at lower fields than H_{a3}. Above $T = 8.5$ K, we observe only the two transitions denoted by H_{a1} and H_{a2}.

3.2.3. Magnetostriction (c-axis). In contrast to the results for the basal-plane axes for which the length decreases with increasing field, the length along the *c*-axis increases

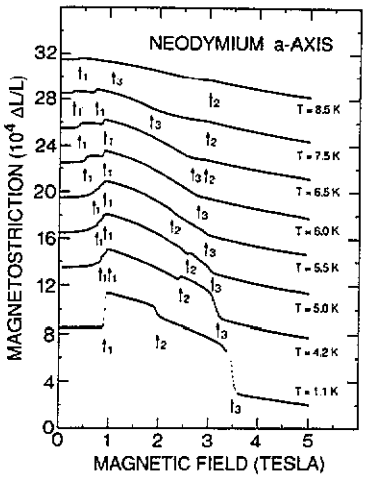

Figure 8. Magnetostriction of Nd, measured in increasing field along the a-axis, for various temperatures. The letter 'i' placed to the right of an arrow refers to the label 'H_{ai}'.

with increasing field. Figure 9 shows three representative results, at $T = 1.5, 7.6$ and 13.5 K. The main feature at 1.5 K is the step-like increase around $H_{c1} = 1.0$ T, which yields a fractional length change approximately half of that measured along the a-axis at H_{a1}. Above H_{c1} there is virtually no magnetostriction until 9 T is applied. It is seen that the response is much more rapid for temperatures below T_3, the temperature at which the moments order on the cubic sites; this suggests that it may be much easier to tilt the cubic moment out of the basal plane, with the implication that the axial anisotropy is greater at the hexagonal sites than at the cubic sites, as deduced previously from elastic constant and neutron diffraction measurements [18, 27, 28].

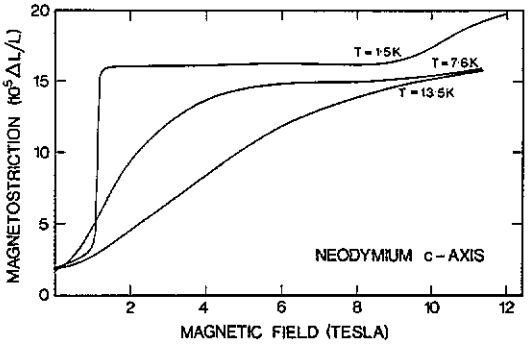

Figure 9. Magnetostriction of Nd, measured in increasing field along the c-axis, for various temperatures.

3.3. Magnetization

Magnetization measurements were made up to $H = 15$ T along the a-, b- and c-axes of the Nd sample. The results are in agreement with earlier measurements up to 5 T

[14,20]. They provide new details which complement pulsed field measurements up to 38 T [29]. For all three orientations of the sample, the magnetization in 15 T has not reached the free-ion value of 3.27 μ_B/atom for Nd. At 4.2 K, for fields along the *b*-axis, the magnetization at $H = 15$ T was 2.09 μ_B/atom. For the *a*- and *c*-axes the corresponding values were 1.96 μ_B/atom and 1.41 μ_B/atom, respectively.

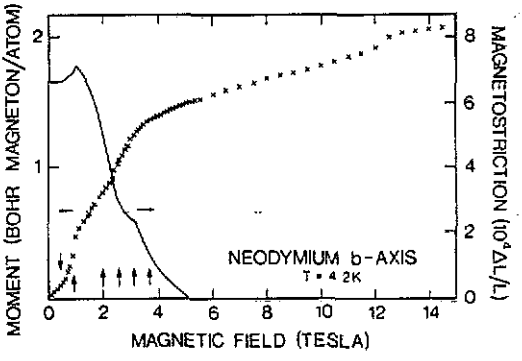

Figure 10. Magnetization and magnetostriction of Nd, measured along the *b*-axis at $T = 4.2$ K. The vertical arrows indicate the positions of the anomalies in the magnetostriction results.

The structure of the observed magnetization curves showed anomalies at fields corresponding to those at which anomalies were seen in the magnetostriction results, as shown in figure 10 for measurements along the *b*-axis at $T = 4.2$ K. This confirms that the anomalies observed in the magnetostriction measurements are due to changes in the magnetic structure of the crystal.

An additional anomaly in the *b*-axis magnetization was observed at high field. At 4.2 K, this anomaly was observed at $H = 12.2$ T (see figure 10). It has also been observed in magnetization measurements along both the *a*- and *b*-axes of a $Nd_{90}Pr_{10}$ sample, but not in $Nd_{75}Pr_{25}$ [30]. In all cases, the position of the anomaly decreased in field with increasing temperatures, but was not followed down into the region accessible in the dilatation experiments.

4. Discussion

The positions of the anomalies seen in the studies mentioned in the introduction are in general agreement with the results of our more comprehensive dilatation studies. We have deduced the magnetic phase diagrams of Nd from the anomalies we have observed, with the results shown in figures 11 and 12 for the *b*- and *a*-axis respectively. The delineated regions of the phase diagram will be interpreted by reference to relevant neutron diffraction investigations.

The first-order transition in zero magnetic field to a single-*q* state at T_N is consistent with the results of the renormalization-group analysis [4]. Furthermore neutron scattering experiments in a magnetic field [6] have identified the region which includes the point $H = 5$ T and $T = 4.2$ K as single-*q*. The dilatation measurements have shown no phase transition within the region labelled single-*q* in figures 11 and 12 so the single-*q* phase can be extended to the interval $T_2 < T < T_N$ at zero magnetic field.

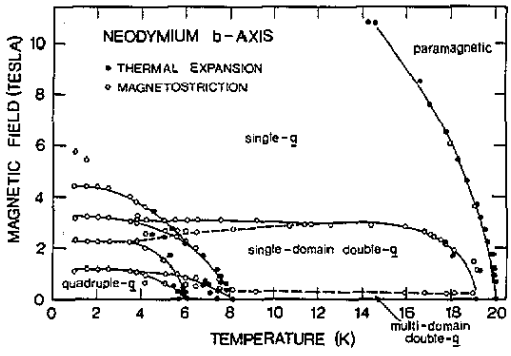

Figure 11. Magnetic phase diagram of Nd, measured with the magnetic field along the *b*-axis.

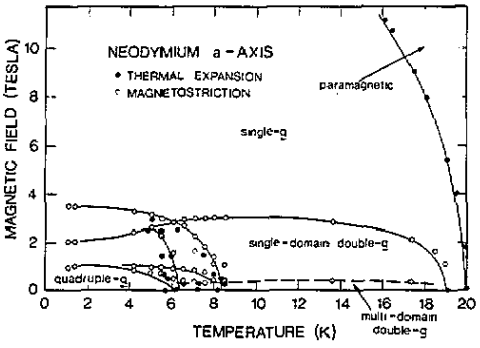

Figure 12. Magnetic phase diagram of Nd, measured with the magnetic field along the *a*-axis.

The Néel temperature decreases with increasing magnetic field for both the *a*- and *b*-axis cases, although the decrease is weaker for fields along the *a*-axis than for fields along the *b*-axis. If we plot the Néel temperature against the square of the applied field along the *a*-axis, as suggested by the free energy analysis [11], we obtain a straight line for temperatures from 19.98 K down to 16 K and for fields from zero to 11 T with a slope $-0.031\ \mathrm{K\,T^{-2}}$. A linear relationship between T_N and H^2 is also observed for fields along the *b*-axis. In this case, however, there is a kink in the line and two linear equations are deduced from the results; for $18.7 < T_N(\mathrm{K}) < 19.9$, i.e., $0.0 < H(\mathrm{T}) < 4.5$, the slope is $-0.063\ \mathrm{K\,T^{-2}}$, while for $14.2 < T_N(\mathrm{K}) < 18.7$, i.e., $4.5 < H(\mathrm{T}) < 11$, the slope of the straight line is $-0.049\ \mathrm{K\,T^{-2}}$.

The kink in the line for the field in the *b*-direction may be explained by the presence of a 'spin–flop' transition near $H = 4.5$ T. In low fields, in the phase below T_N where the single-*q* state exists, the moments S_1, S_2, and S_3 lie along the three equivalent *b*-directions. As the field is increased, parallel to S_1, the $(m\cdot S_i)^2$ terms in the free energy [11] become important and eventually S_2 and S_3 are driven perpendicular to the field direction. We suggest that this occurs at 4.5 T, the field at which the kink occurs in the T_N versus H^2 line. In the case of the *a*-axis field, only domains where the spin is perpendicular to the field are selected.

The phase boundary which begins at T_2, $H = 0$ T, and rises to approximately $H = 3$ T can be identified with the transition from a single-domain double-*q* structure

to a single-domain single-q structure. Such a transition, labelled H_{b3} in figure 7 and H_{a2} in figure 8, has been observed [6] in neutron diffraction studies in a magnetic field at a temperature of 14 K. For both the a- and b-axes the phase boundary can be followed down to $T = 1$ K, as it crosses the phase boundaries emanating from T_3 and T_5. In the case of the a-axis, the transition has been followed smoothly to 2.0 T. However, the b-axis results indicate the presence of an intermediate phase between the double-q and single-q regions. The splitting of the H_{b3} phase boundary begins at 11.5 K: the lower boundary (denoted by $H_{b2'}$ and observed in decreasing-field results as well) may be followed down in temperature until it merges with the transition labelled H_{b2} (see figure 11). This intermediate phase was not detected in the neutron study [6]. However, this may well have been because the field was applied some 5° away from a b-direction, in order to facilitate the formation of a single domain single-q state, whereas in the experiments reported here, the field was applied along the symmetry direction, with an accuracy of $\frac{1}{2}°$ to 1°. As with all of the phase lines drawn on figures 11 and 12, these boundaries become nearly horizontal to the T-axis at low T, consistent with the third law of thermodynamics.

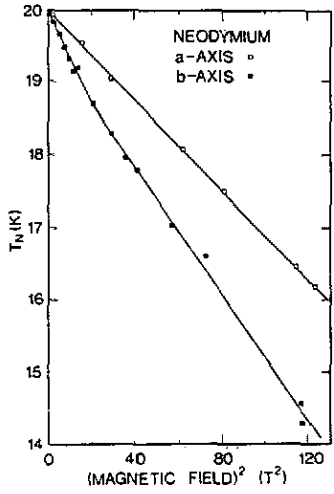

Figure 13. T_N versus H^2 for magnetic fields along the a- and b-axes of Nd.

The delineation of the low-temperature phases in the *(H,T)* diagrams can best be seen at $T \approx 1.8$ K. A recent neutron diffraction study has been made of the low-temperature phases of Nd at temperatures $T > 1.8$ K and in fields $H < 5.0$ T, applied 5° from a ⟨100⟩ axis [31,32]. Consider the b-axis phase diagram and figure 14, a schematic representation of the modulation wavevectors associated with the various phases. In zero field at 1.8 K the quadruple-q structure exists, with q_1 and q_2 associated with the hexagonal sites and q_3 and q_4 with the cubic sites. At $T = 1.8$ K and $H = 0.8$ T the neutron diffraction experiments show that the quadruple-q phase is replaced by a triple-q phase in which there is only one wavevector associated with the cubic sites and the longitudinal splitting of the hexagonal modulation wavevectors gives way to two wavevectors, q_1 and q_2, of equal length. The position of an additional peak at $0.063\tau_{100}$ corresponds to that of the subharmonic $q_1/2$. The transition labelled $H_{b1'}$ in figure 7 marks the onset of this phase. The diffraction pattern

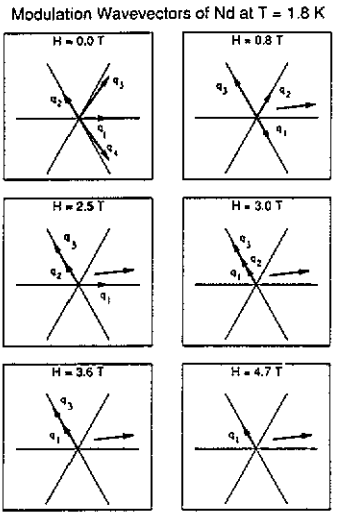

Figure 14. A schematic representation of the wavevectors associated with the various magnetic phases of Nd at $T \approx 1.8$ K. The arrow indicates the direction of the applied magnetic field.

at 2.0 T clearly shows the intermodulation harmonics of the type $2q_1 \pm q_2$ but the subharmonic $q_1/2$ is no longer apparent. We propose that H_{b1} marks the transition to this phase. Above $H_{b2} \approx 2.2$ T one of the hexagonal wavevectors moves parallel to the field direction whilst the intensity of the cubic satellite has diminished. However the subharmonic at $q_1/2$ has reappeared.

By $H \approx 3.0$ T the hexagonal satellites are again positioned *longitudinally* on the $\langle 100 \rangle$ axis, with the magnitudes of q_1 and q_2 being 0.105 and $0.116|\tau_{100}|$, i.e., they have regained their zero-field values. Furthermore, the neutron diffraction study reveals the dramatic appearance of a sequence of harmonics and subharmonics of q_1 in a series of peaks at $2q_1$ and $3q_1$ as well as at $q_1/2$, $3q_1/2$ and $5q_1/2$ and also $q_1/4$ and $3q_1/4$ [31]. This so-called *archipelago phase* seems to be related to the co-existence of a single-q cubic wavevector and hexagonal wavevectors which are along the same symmetry direction. The difference in length between this phase and that at 2.5 T must be minimal since no anomalies are observed in the magnetostriction measurements. The transition at $H_{b3} \approx 3.3$ T marks the disappearance of the q_2 wavevector with no qualitative changes in the harmonics and subharmonics of q_1.

Finally, at $H = 4.7$ T, i.e., above $H_{b4} = 4.4$ T, the cubic ordering has disappeared, leaving only a single hexagonal wavevector at $q_1 = 0.113\tau_{100}$ with an associated $3q_1$ harmonic and $q_1/2$ subharmonic present in the diffraction pattern.

An anomaly observed in neutron diffraction measurements at $H = 2.6$ T, along the a-axis, was attributed to a large increase (a 67% increase on the cubic sites and a 160% increase on the hexagonal sites) in the ferromagnetic moments on the two sites

[12]. Although magnetization measurements in this and another study [20] indicate the existence of anomalies near $H = 2.6$ T, they do not show comparable increases in the moment when the fields were directed in either the a- or b-axis, as demonstrated in figure 10.

Both figures 11 and 12 show phase boundaries which originate in zero field from $T_3 = 8.2$ K, the temperature at which the satellites at $q_c = 0.18\tau_{100}$ appear. The phase diagrams indicate that these satellites, which arise primarily from the ordering of the moments on the cubic sites, exist within the boundaries labelled by H_{a3} and H_{b4}, for the a-and b-axes, respectively. Neutron diffraction experiments showed that the single-q_c phase was eliminated by a field of 3.2 T applied along an a-axis at 4.2 K [12], and by 4.5 T applied along a b-axis at 1.8 K [31]; it is proposed that the upper line from T_3 delineates the extent of the single-q_c phase. This upper line can be traced down to $T = 1$ K where it is found near $H = 4.4$ T for the b-axis and $H = 3.5$ T for the a-axis. Recent measurements between T_3 and T_5 show a triple-q phase in which a single modulation wavevector associated with the cubic sites bisects q_1 and q_2 [31].

The temperature $T_5 \approx 6.2$ K corresponds to the longitudinal splitting of the *hexagonal* wavevector into the on-axis q_1 and q_2 and the transverse splitting of the *cubic* wavevector into the off-axis q_3 and q_4, or the quadruple-q phase. In zero field this phase has six domains [7] and so a neutron diffraction pattern of 36 satellites is observed, as discussed earlier. At this temperature, the coupling term $(q_i \cdot S_i)^2$, which drives the single-q to double-q transition at T_2 [11], apparently has less significance for the hexagonal sites where the wavevectors align themselves with the $\langle 100 \rangle$ direction than for the cubic sites where the wavevectors have moved away from the symmetry directions. Interestingly, it has been observed that an addition of 10% Pr to Nd creates a situation where 48 magnetic satellites are seen, i.e., the hexagonal wavevectors have moved away from $\langle 100 \rangle$ [33]. The transverse splitting of the cubic satellites—the emergence of q_3 and q_4—is suppressed by fields of less than 1 T [27] and it is proposed that the anomaly at 4.2 K at $H_{b1'}$ is between double-q and single-q structures on the cubic sites. It is also proposed that the upper phase boundary emerging from T_5, which terminates at the hexagonal double-q to hexagonal single-q line in the phase diagrams signifies a transition on the hexagonal layers (with decreasing temperature) from a double-q structure in which the wavevectors are tilted *away* from the symmetry directions to one in which they are *parallel* to the symmetry directions. It has been observed that the cubic satellites split in a direction perpendicular to the basal plane at temperatures near this phase line [34].

A feature of all the magnetostriction results below 10 K is the increase in length at H_{a1} and H_{b1} which is at or below $H = 1$ T. After this transition, $\Delta L/L$ predominantly decreases. In this region of decreasing length, which can be attributed to the formation of an induced ferromagnetic moment [12], there are a series of anomalies. For the b-axis these include H_{b2} to H_{b4} at 1 K to H_{b3} alone at 9.2 K and higher temperatures. Positive length increases are only observed at the transitions $H_{b2'}$ over the region $T = 4.2$ to 6.5 K and H_{a2} from $T = 4.2$ to 5.0 K.

A partial phase diagram has been constructed previously from anomalies in magnetization measurements along the b-axis [20]. The results below $H = 1$ T agree well with those of this study, but there are some discrepancies at higher fields. In particular, the phase diagram of [20] shows a splitting of the $H = 3$ T phase boundary only below 9 K. Our results also show a splitting, of approximately the same magnitude, which can be followed from $T = 11.5$ K down to 1 K. The origin of this split phase

boundary (which does not exist in the phase diagram for the a-axis) may be due to the re-orientation of the double-q wavevectors with respect to the symmetry axes. Indeed, neutron diffraction results in this region [31] suggest a precursor phase to the single-q phase in high fields.

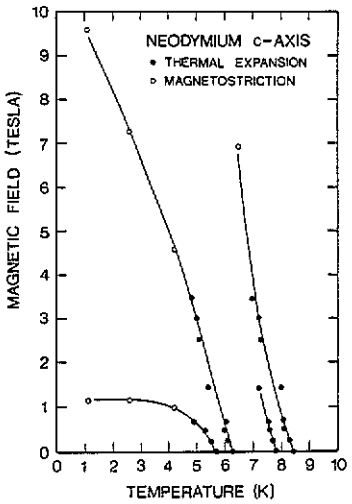

Figure 15. Magnetic phase diagram of Nd, measured with the magnetic field along the c-axis.

The anomalies observed in measurements along the c-axis have been used to produce the magnetic phase diagram for this direction (see figure 15). Four phase boundaries are evident. The first line begins at $T_3 = 8.4$ K at $H = 0$ T and rises through $H = 7$ T at $T = 6.4$ K. This line corresponds to the appearance of magnetic satellites at $0.18\tau_{100}$. Another line, parallel to the first one but displaced by 0.5 K, was observed only at fields below 2 T. The third phase boundary has its origin at $T_5 = 6.3$ K and rises rapidly with field; it corresponds to the onset of the quadruple-q phase, i.e., the longitudinal splitting of the neutron diffraction satellites on the hexagonal sites. The last phase boundary observed along the c-direction begins at $T_6 = 5.7$ K and rises to $H = 1.2$ T where it flattens out; it is proposed that this line corresponds to the movement of q_c out of the basal plane [34].

5. Conclusions

The measurement of length changes in Nd has proven to be a valuable technique in discerning the sequence of increasingly complex magnetic structures below T_N. The magnetic phase diagrams deduced from the dilatation results reported here provide a valuable guide to regions of *(H,T)* space which require detailed examination in neutron diffraction studies. Although great progress has been made, further studies are required to complete our understanding of the low-temperature transitions. Attention should be given to the phases below 1 T, where the interaction between the hexagonal and cubic sites dominates. This is especially important near 6 K where one of the phase boundaries appears to be correlated with the movement of moments out of the basal plane. Further investigation should also be made on the phase boundary

splittings with 3 T applied along the *b*-axis. Also, the association of cubic site ordering with the occurrence of the *archipelago* phase needs to be examined more closely. Measurements made with the field along the *c*-axis at $T < 10$ K would help clarify the interaction of the moments in the basal plane with those along the *c*-axis.

Acknowledgments

This work was partly supported by a NATO Research Grant and by the SERC. We acknowledge helpful discussions with E M Forgan and M B Walker. We are most grateful to D Fort for preparing the single crystal used in this experiment. We are also grateful to M Picoche and the SNCI, Grenoble for making their facilities available for the magnetization measurements.

References

[1] Parkinson D H, Simon F E and Spedding F H 1951 *Proc. R. Soc.* A **207** 137
[2] Moon R M, Cable J W and Koehler W C 1964 *J. Appl. Phys.* **35** 1041
[3] Lebech B 1981 *J. Appl. Phys.* **52** 2019
[4] Bak P and Lebech B 1978 *Phys. Rev. Lett.* **40** 800
[5] Forgan E M 1982 *J. Phys. F: Met. Phys.* **12** 779
[6] McEwen K A, Forgan E M, Stanley H B, Bouillot J and Fort D 1985 *Physica* B **130** 360
[7] Forgan E M, Gibbons E P, McEwen K A and Fort D 1989 *Phys. Rev. Lett.* **62** 470
[8] Zochowski S and McEwen K A 1986 *J. Magn. Magn. Mater.* **54–57** 515
[9] Lebech B, Als-Nielsen J and McEwen K A 1979 *Phys. Rev. Lett.* **43** 65
[10] Walker M B and McEwen K A 1983 *J. Phys. F: Met. Phys.* **13** 139
[11] McEwen K A and Walker M B 1986 *Phys. Rev.* **B34** 1781
[12] Lebech B and Rainford B D 1974 *Proc. Int. Conf. on Magnetism, Moscow* vol 3 (Moscow: Nauka) p 191
[13] Gibbons E P 1989 *PhD Thesis* University of Birmingham
[14] Johansson T, Lebech B, Nielsen M, Moller H B and Mackintosh A R 1970 *Phys. Rev. Lett.* **25** 524
[15] McEwen K A 1986 unpublished
[16] Forgan E M, Muirhead C M, Jones D W and Gschneidner K A 1979 *J. Phys. F: Met. Phys.* **9** 651
[17] Lenkkeri J T and Palmer S B 1977 *J. Phys. F: Met. Phys.* **7** 15
[18] Palmer S B and Lenkkeri J T 1978 *J. Phys. F: Met. Phys.* **8** 1359
[19] Boghossian H and Coles B R 1982 *J. Magn. Magn. Mater.* **29** 213
[20] Boghosian H H, Coles B R and Fort D 1985 *J. Phys. F: Met. Phys.* **15** 953
[21] Willemson H W, Martin C A, Meincke P M and Armstrong R L 1977 *Phys. Rev.* B **16** 2883
[22] Steinitz M O, Willemson H and Britton D private communication
[23] White G K 1961 *Cryogenics* **1** 151
[24] Gibbons E P 1987 *MSc Thesis* University of Birmingham
[25] Kroeger F R and Swenson C A 1977 *J. Appl. Phys.* **48** 853
[26] Johansson T, McEwen K A and Toubourg P 1971 *J. Physique Coll.* **32** C1 372
[27] Lebech B and Rainford B D 1971 *J. Physique Coll.* **32** C1 370
[28] Stanley H B, Brown P J, McEwen K A and Rainford B D 1986 *Physica* B **136** 400
[29] McEwen K A, Cock G J, Roeland L W and Mackintosh A R 1973 *Phys. Rev. Lett.* **30** 287
[30] Zochowski S W and McEwen K A to be published
[31] McEwen K A and Zochowski S W 1990 *J. Magn. Magn. Mater.* **90–91** 94
[32] Forgan E M, Lee S L, Marshall W G, McEwen K A and Zochowski S W 1991 *Proc. Int. Conf. on Magnetism (Edinburgh), J. Magn. Magn. Mater.* at press
[33] Zochowski S W, McEwen K A and Forgan E M 1991 *Proc. Int. Conf. on Neutron Scattering (Oxford), Physica* B at press
[34] Forgan E M, Lee S L, and Zochowski S W 1991 *Proc. Int. Conf. on Magnetism (Edinburgh), J. Magn. Magn. Mater.* at press